Structural transformation of MnO_2 during the oxidation of bisphenol A

Sarah Balgooyen,[1] *Peter J. Alaimo,*[2]

Christina K. Remucal, [1, 3]† *and Matthew Ginder-Vogel,*[1,3]*

[1]Environmental Chemistry and Technology Program

University of Wisconsin – Madison

Madison, Wisconsin

[2]Department of Chemistry

Seattle University

Seattle, Washington

[3]Department of Civil and Environmental Engineering

University of Wisconsin – Madison

Madison, Wisconsin

Submitted to: *Environmental Science and Technology,* November 22, 2016.

Contents (27 pages): Figures: S1-S16, Tables: S1-S4

† Corresponding author address: 660 N. Park St., Madison, WI 53706; e-mail: remucal@wisc.edu; telephone: (608) 262-1820; fax: (608) 262-0454; Twitter: @remucal.

* Corresponding author address: 660 N. Park St., Madison, WI 53706; e-mail: mgindervogel@wisc.edu; telephone: (608) 262-0768; fax: (608) 262-0454; Twitter: @profmattgv.

Table of Contents

S1: Materials

Acetonitrile (HPLC grade), methanol (HPLC grade), formic acid (ACS, 88%), calcium chloride dihydrate (ACS, 100%), and potassium permanganate (ACS), were purchased from Fisher Chemical. Bisphenol A (≥99%) and L-ascorbic acid (≥99%) were purchased from Sigma-Aldrich. Manganese(II) nitrate tetrahydate (analytical grade), piperazine-*N,N'*-bis(2-ethanesulfonic acid) (PIPES, 99%), and sodium oxalate (98.5%) were purchased from Acros Organics. Boron nitride (99.5%, 325 mesh) was purchased from Alfa Aesar. Sodium hydroxide (98%) was purchased from Sigma Chemical Co.

Preparation of 4-Hydroxycumyl Alcohol (HCA). This synthesis (Figure **S1**) is a modification of the method reported by Nakamura *et al.*,[1] and provides a significantly improved yield. A 100-mL round bottom flask charged with a teflon-coated stirbar was oven-dried overnight, fitted with a rubber septum, and cooled to room temperature under a stream of nitrogen gas. The flask was charged with *p*-acetoxyacetophenone (1.04 mL; 6.6 mmol) and dry Et_2O (20 mL). The mixture was cooled to 0°C in an ice bath. A solution (3M in Et_2O) of methylmagnesium iodide (7.0 mL; 21 mmol) was added dropwise over 5 min, resulting in formation of a yellow precipitate. The ice bath was removed and the mixture was allowed to warm to room temperature with stirring overnight. The reaction was opened up to air and quenched by the slow addition of aqueous ammonium chloride (saturated, 100 mL). The mixture was extracted using EtOAc (3 x 35 mL). The combined organic layers were washed with brine (35 mL), dried over $MgSO_4$, and filtered. The volatile materials were removed *in vacuo* to afford a pink-colored residue. The product was crystallized from hot EtOAc to give 4-hydroxycumyl alcohol (924 mg; 6.07 mmol; 92 % yield) as a white powder.

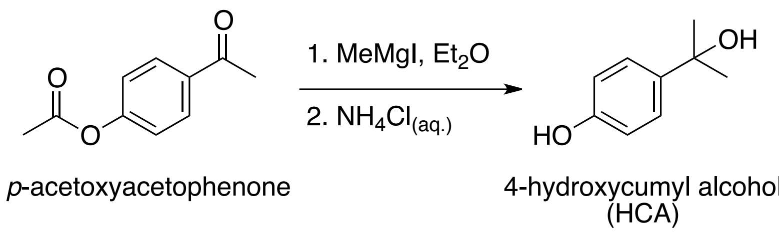

Figure S1. Synthesis reaction of HCA.

^{1}H NMR (400 MHz, CD_3OD): δ 7.28 (d, *J* = 8 Hz, 2H), 6.71 (d, *J* = 8 Hz, 2H), 1.48 (s, 6H) ppm. This matches the literature characterization.[1]

^{13}C NMR (100 MHz, CD_3OD): δ 156.8, 141.7, 127.0, 115.4, 72.7, 31.9 ppm.

IR (KBr pellet): ν 3394, 3128, 2971, 2682, 2592, 2499, 1890, 1612, 1597, 1516, 1466, 1448, 1397, 1379, 1303, 1239, 1179, 1160, 1111, 1102, 1016, 956, 935, 861 cm^{-1}.

LRMS (Agilent 6460 triple quadrupole, electrospray ionization, negative mode) calculated *m/z* for $C_9H_{12}O_2$: 152.08; found *m/z* 151.10 [M-H]$^-$, 133.10 [M-H_3O)$^-$ (Figure S2). This matches the literature characterization.[2]

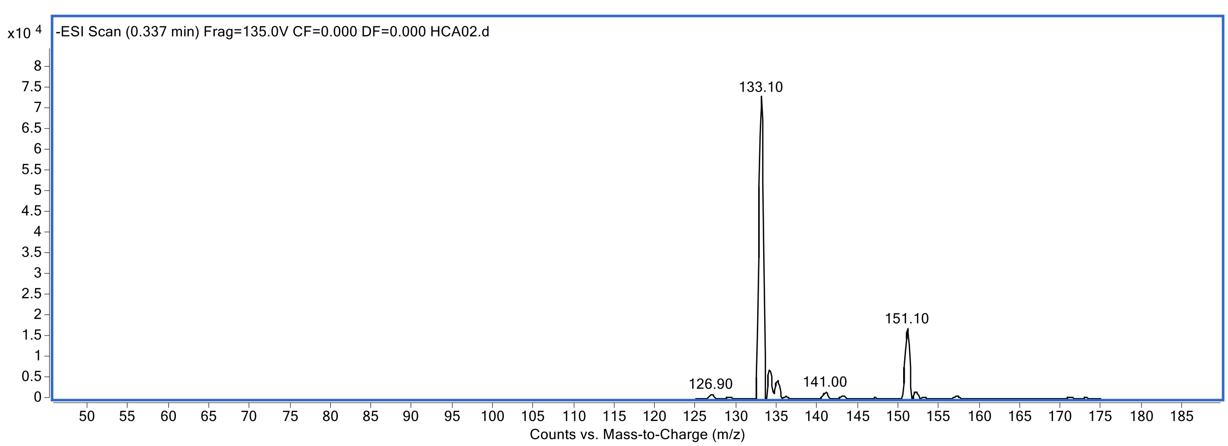

Figure S2. Mass spectrum of synthesized HCA collected using an Agilent triple quadrupole LC-MS with electrospray ionization in negative mode. Molecular ion = 151.10; base peak = 133.10.

S2: Analytical Methods

High Performance Liquid Chromatography (HPLC) Analysis. HPLC analyses were performed with an Agilent 1260 instrument equipped with a fluorescence detector (Model 1260 FLD) and a UV detector (Model 1260 DAD). The peaks detected in experimental chromatograms were compared to authentic standards.

Column:	Agilent Poroshell 120 EC-C18 (4.6 x 50 mm, 2.7 μm)	
Guard column:	Agilent EC-C18 (3.0 x 5 mm, 2.7 μm)	
Injection volume:	5 μL	
Mobile phase:	A: 0.1% Formic Acid + 10% Acetonitrile (ACN) in Milli-Q water adjusted to pH 3 (filtered through a 0.2 μm nylon filter)	
	B: 100% ACN	
Flowrate:	0.6 mL/min	
Column temperature:	$30^{o}C$	
Isocratic:	% Solvent A	% Solvent B
	60	40
Method duration:	6.00 min	

Target Analyte	Excitation Wavelength (nm)	Emission Wavelength (nm)	Retention Time (min)
BPA	280	310	2.65
HCA	280	310	0.66

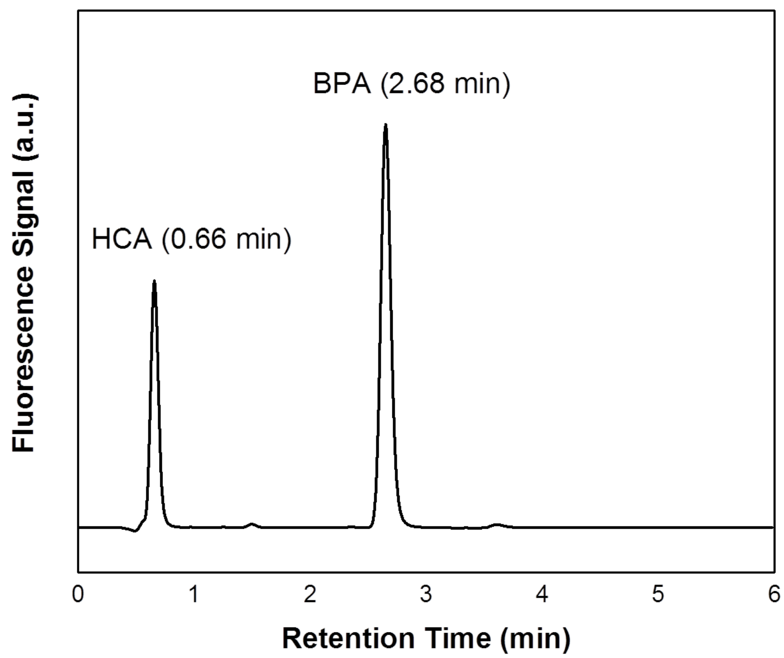

Figure S3. HPLC chromatogram of a sample from the 12-addition experiment of 80 μM BPA with 0.33 g/L Mn(III)-rich δ-MnO_2 in PIPES buffer (pH 7).

Inductively Coupled Plasma-Optical Emission Spectroscopy (ICP-OES) Analysis. ICP-OES analyses were performed on a PerkinElmer Optima 4300 DV to quantify aqueous manganese in the reactors at various time intervals. All samples were filtered immediately and diluted in a solution of 2% nitric acid. Standards were made from a SPEX CertiPrep 1000 mg/L Mn stock diluted in 2% nitric acid. Error was calculated using relative standard deviations from four instrument responses.

S3: Rate Constant Analysis

Rate constants for the oxidation of BPA and HCA by Mn oxides were calculated assuming pseudo-first-order kinetics according to:

$$\ln[A] = -kt + \ln[A]_o \qquad \textbf{S1}$$

where A is the concentration of the organic (M), t is the time of the reaction (min), and k is the rate constant (min^{-1}). Since the reaction deviates from pseudo-first-order kinetics after long reaction durations, only data from the linear portion of these plots were used to calculate rate constants (R^2 ≥0.98 for the first 4 additions, R^2 ≥0.90 for additions 5-12). Reported rate constants are averages of rate constants calculated at multiple time points. For example, the data in Figure S4a would be used to calculate an average rate constant by using the rate constant in the first two minutes, the first three minutes, and the first four minutes. This method was used in order to provide an average and standard deviation of the rate constant throughout each reaction of BPA with MnO_2. As shown in Figure S4b, the data deviates from pseudo-first-order regime after a certain time point, and these later time points are not used in rate constant calculations or error determination. The error for each rate constant is the standard deviation of the rate constants collected at all useable time points. Half-lives ($t_{1/2}$) were calculated using equation S2:

$$t_{1/2} = \frac{\ln(2)}{k} \qquad \textbf{S2}$$

The reaction length of each addition was based on estimation to capture as much of the degradation process as possible. The first several reactions were designed to allow enough time to oxidize the entire aliquot of BPA.

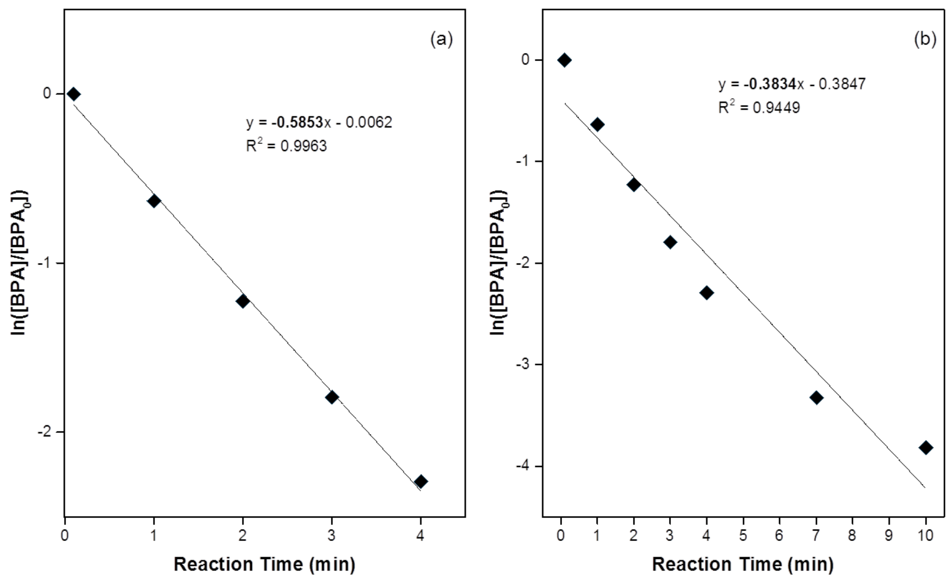

Figure S4. Pseudo-first-order rate analysis of (a) the first four minutes and (b) the first ten minutes of 80 μM BPA oxidation by 0.33 g/L Mn(III)-rich δ-MnO_2 in PIPES pH 7.

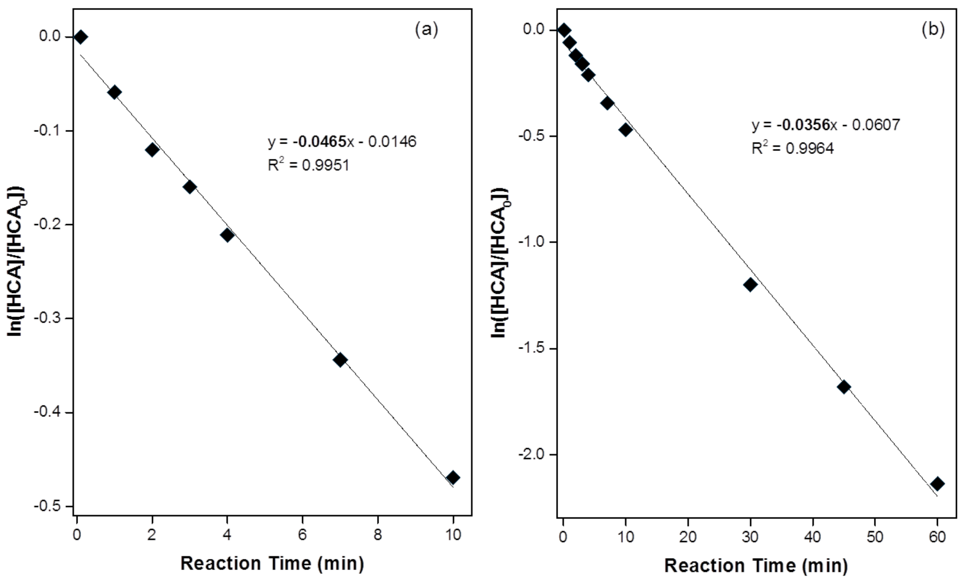

Figure S5. Pseudo-first-order rate analysis of (a) the first 10 minutes and (b) the first 60 minutes of 80 μM HCA oxidation by 0.33 g/L Mn(III)-rich δ-MnO_2 in PIPES pH 7.

S4: HCA Detection and Yield Calculation

HCA Identification. The oxidation product in this reaction was identified as HCA by comparing its UV spectrum and HPLC retention time to pure HCA synthesized as described in Section S1. The UV spectra of the BPA product aligned with that of the synthesized HCA, with λ_{max} of both compounds occurring at 221 nm and 260 nm (Figure **S6**). The molar extinction coefficient of HCA at 221 nm is 7173.5 M^{-1} cm^{-1} at pH 7. The retention times of both the authentic standard and the oxidation product were at 0.657 min using the HPLC method described in Section S2 (Figure **S7**).

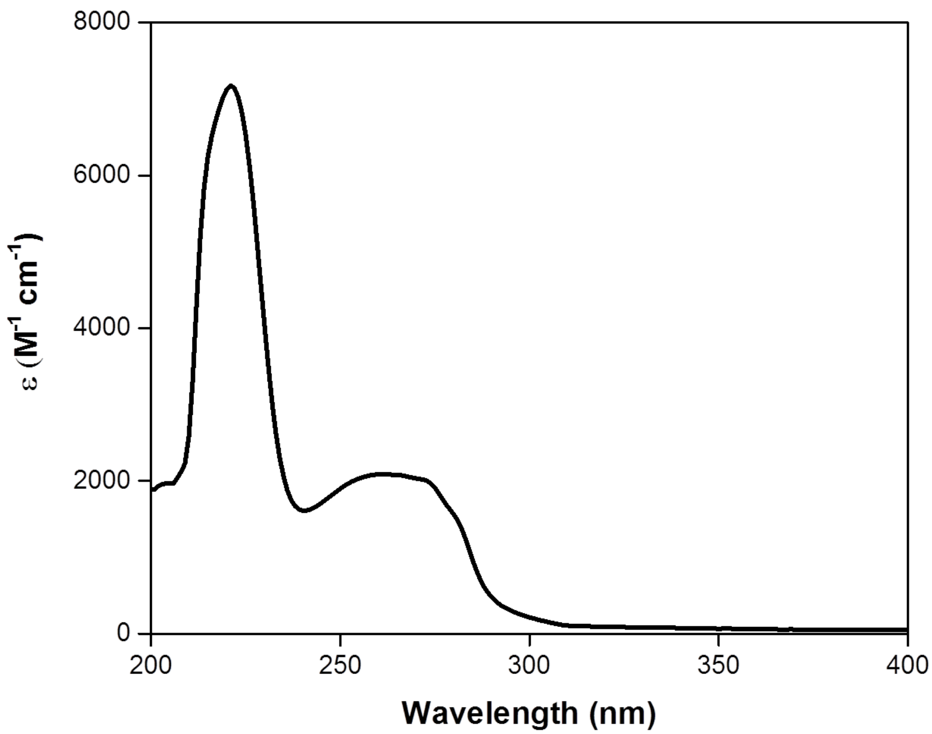

Figure S6. UV spectrum of the synthesized HCA at pH 7.

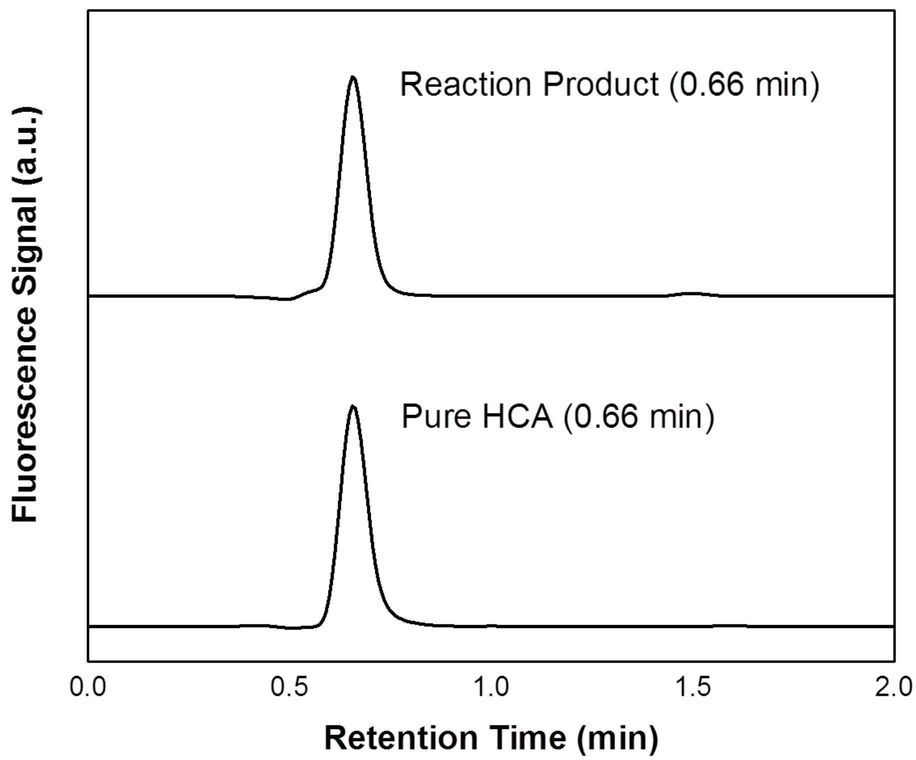

Figure S7. HPLC chromatograms of the synthesized HCA and reaction products, measured using a fluorescence detector.

HCA Quantification. The rate of change of BPA with time was modeled by assuming pseudo-first-order kinetics according to:

$$\frac{\mathrm{d[BPA]}}{\mathrm{dt}} = -k_1[\mathrm{BPA}] \qquad \mathbf{S3}$$

where [BPA] is the concentration of BPA at time t and k_1 is the measured pseudo-first-order loss rate of BPA. This differential expression integrates to:

$$[\mathrm{BPA}] = [\mathrm{BPA}]_0 \mathrm{e}^{-k_1 \mathrm{t}} \qquad \mathbf{S4}$$

where $[BPA]_0$ is the initial concentration of BPA.

The differential expression describing the change in HCA concentration with time is given by:

$$\frac{d[HCA]}{dt} = k_1 F_{HCA}[BPA] - k_2[HCA] \qquad \textbf{S5}$$

where [HCA] is the concentration of HCA at time *t* and F_{HCA} is the yield of HCA from BPA oxidation. k_2 is the pseudo-first-order loss rate of HCA, which is assumed to be 12.6 times slower than k_1 based on control experiments (Figures **S4** and **S5**). Equation S5 can then be integrated to give an expression of the form:

$$[HCA] = \frac{k_1 F_{HCA}[BPA]_{\mathbf{0}}}{\boldsymbol{k_1 - k_2}} \left(e^{-k_1 t} - e^{-k_2 t}\right) \qquad \textbf{S6}$$

F_{HCA} is then determined by fitting the measured HCA concentrations according to equation S6, which is identical to equation 1 in the manuscript.

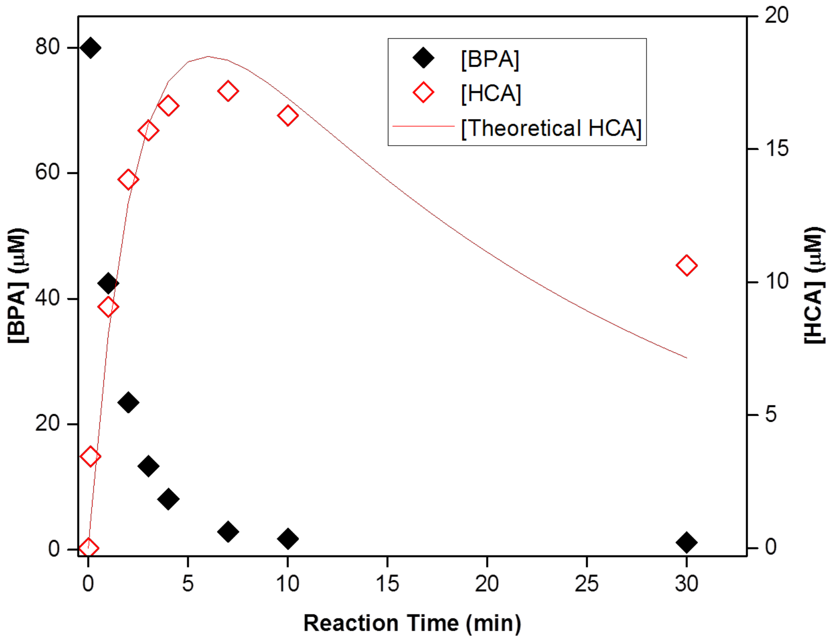

Figure S8. A sample single-addition batch reaction of 80 μM BPA with 0.33 g/L Mn(III)-rich δ-MnO_2 in PIPES pH 7 buffer. Theoretical HCA production is modeled using a least-squares minimization with Equation **1** in the manuscript and the measured data set.

Table S1. Percentages of BPA recovered as HCA on a molar basis during each of the twelve additions of 80 µM BPA to 0.33 g/L Mn(III)-rich δ-MnO_2, calculated using Equation **1**.

Additions of BPA	HCA Yield (% of BPA)
1	39.73
2	42.31
3	35.63
4	21.33
5	17.80
6	5.63
7	2.63
8	2.98
9	2.42
10	3.58
11	1.86
12	3.54

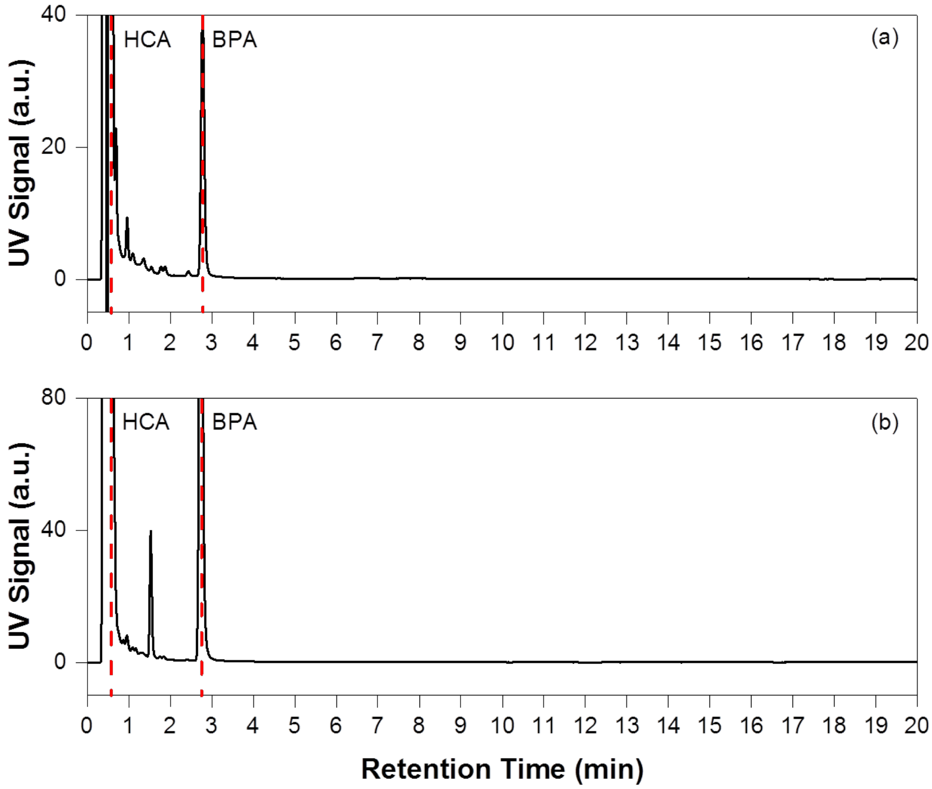

Figure S9. HPLC chromatograms using a DAD detector (230 nm) from (a) the first minute of the first addition, and (b) the last minute of the twelfth addition during twelve additions of 80 µM BPA with 0.33 g/L Mn(III)-rich δ-MnO_2 in PIPES pH 7 buffer.

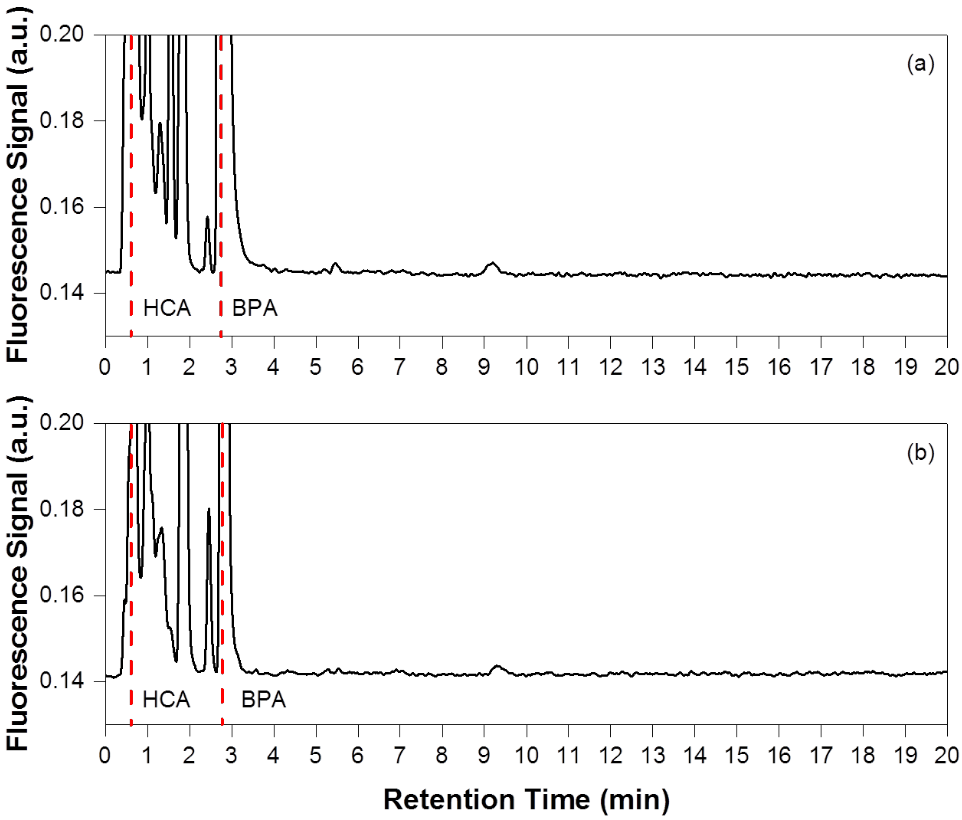

Figure S10. HPLC chromatograms using an FLD detector from (a) the first minute of the first addition, and (b) the last minute of the twelfth addition during twelve additions of 80 μM BPA with 0.33 g/L Mn(III)-rich δ-MnO_2 in PIPES pH 7 buffer.

S5: Sorption Analysis

Table S2. The percentages of BPA and HCA sorbed during three sequential additions of 80 μM BPA to 0.33 g/L Mn(III)-rich δ-MnO_2 in PIPES pH 7 buffer. All reactions were 60 minutes in duration.

BPA Addition		
# of BPA Additions	**% BPA Sorbed**	**% HCA Sorbed**
1	14.3 ± 7.4	0 ± 0
2	0 ± 0	0.9 ± 1.4
3	0.2 ± 0.5	1.0 ± 0.9

S6: Solids Analysis

Table S3. BET analysis of surface area in a subset of solids collected after each addition.

Surface Analysis	
# of BPA Additions	**Surface Area (m^2/g)**
0	118 ± 15
3	100 ± 15
6	106 ± 15
9	124 ± 15

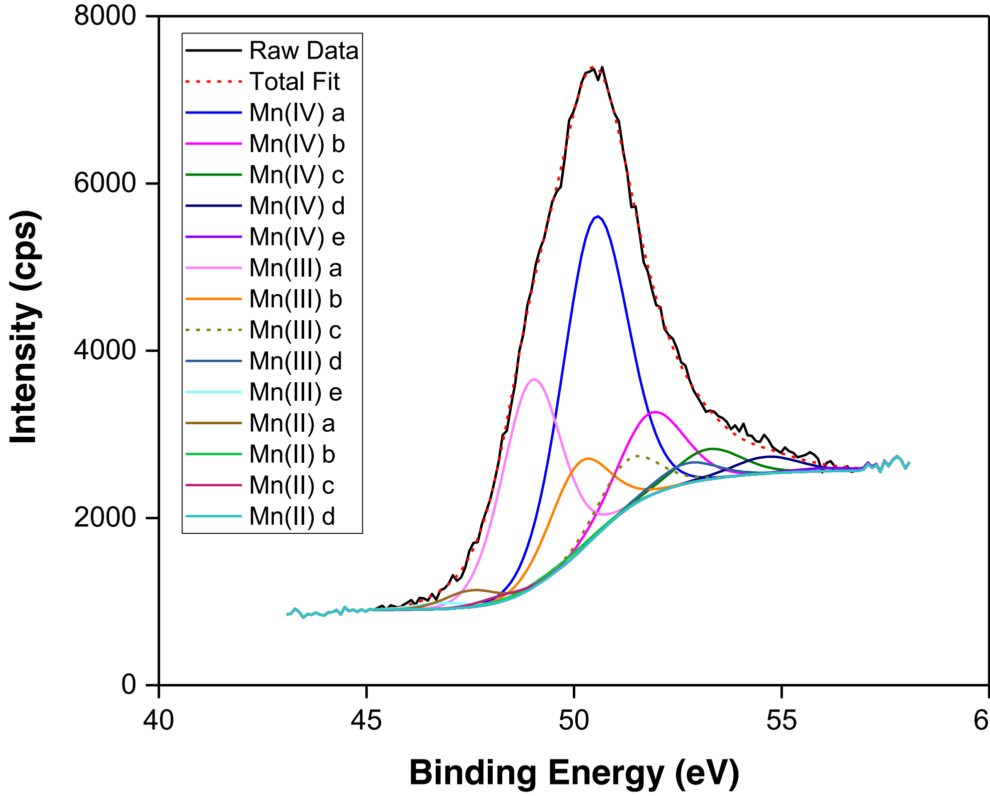

Figure S11. Fitted XPS data from the starting material using the method described in the Materials and Methods section of the manuscript. Uncertainty in the mole fraction is ±0.02 for Mn(IV) and Mn(III) and ±0.01 for Mn(II).

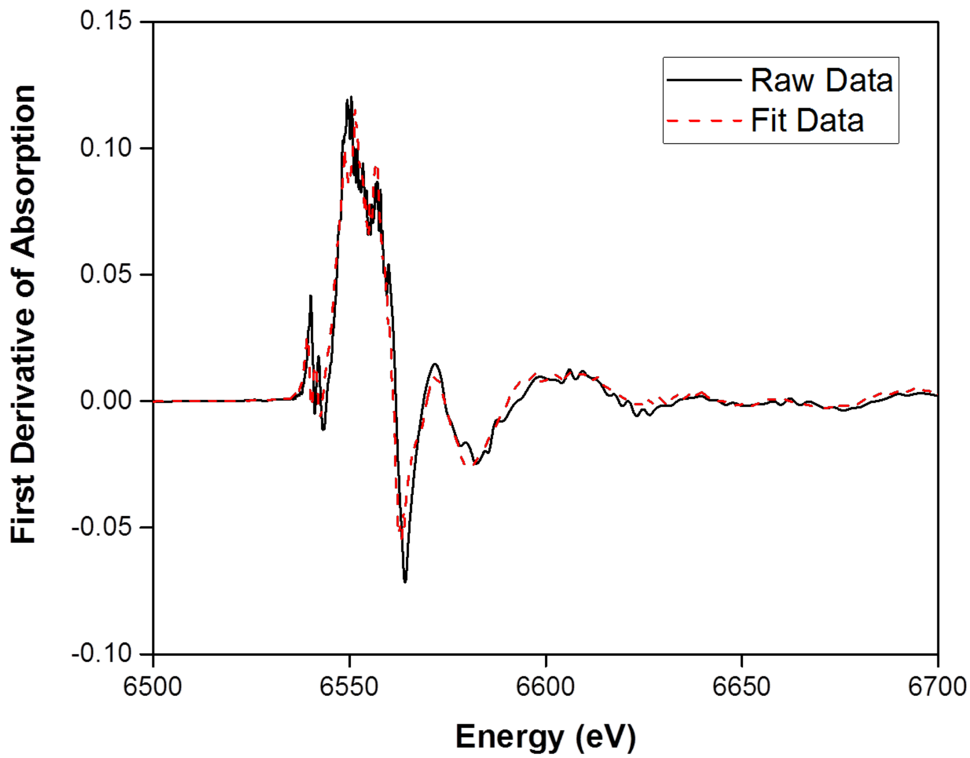

Figure S12. Fitted XANES data from the starting material using the Combo method described in the Methods and Materials section of the manuscript.

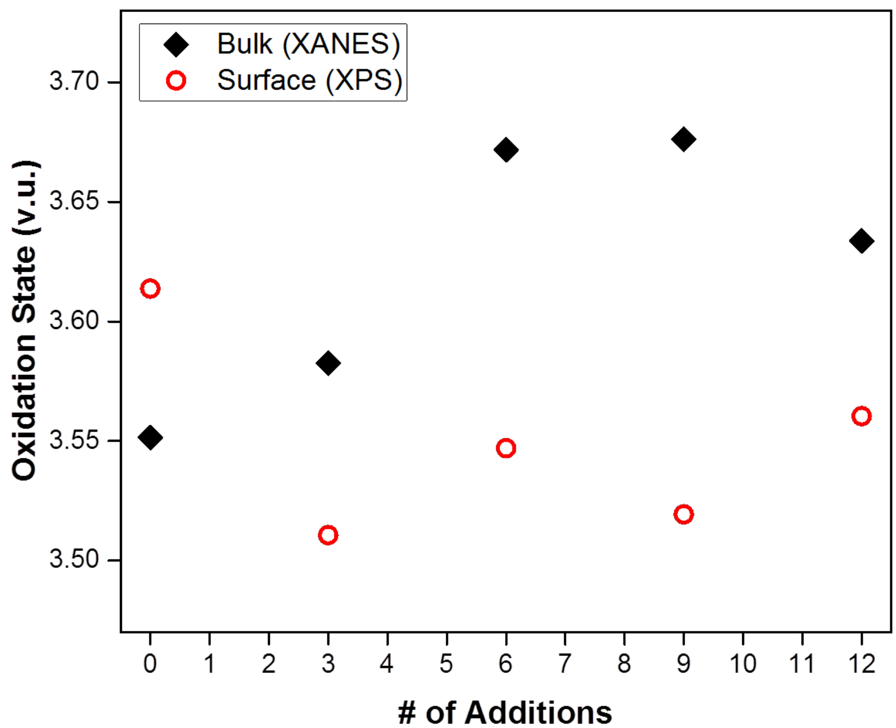

Figure S13. Oxidation state (measured by XANES and XPS) of a subset of solid samples over twelve additions of 80 µM BPA with 0.33 g/L of Mn(III)-rich δ-MnO_2 in a PIPES pH 7 buffer. Data is an average of two reactors.

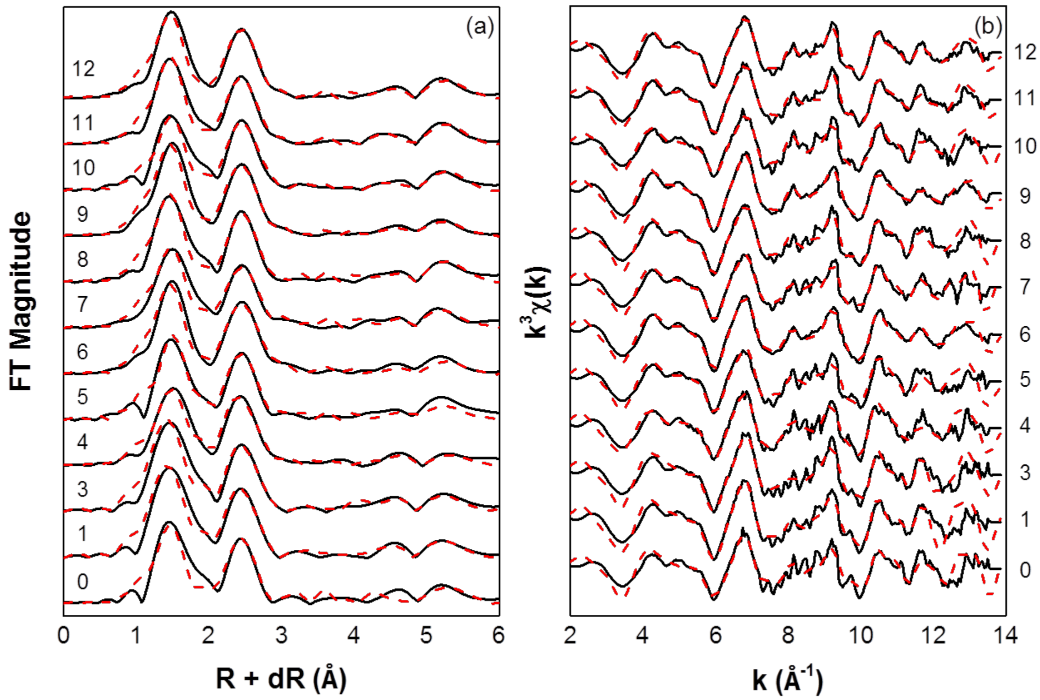

Figure S14. Raw and modeled data of (a) the chi functions and (b) relative radial distribution function from EXAFS analysis of solids over twelve additions of 80 μM BPA with 0.33 g/L of Mn(III)-rich δ-MnO_2 in a PIPES pH 7 buffer. The addition number is indicated by the numbers next to each data set. Samples from both reactors were combined and then analyzed.

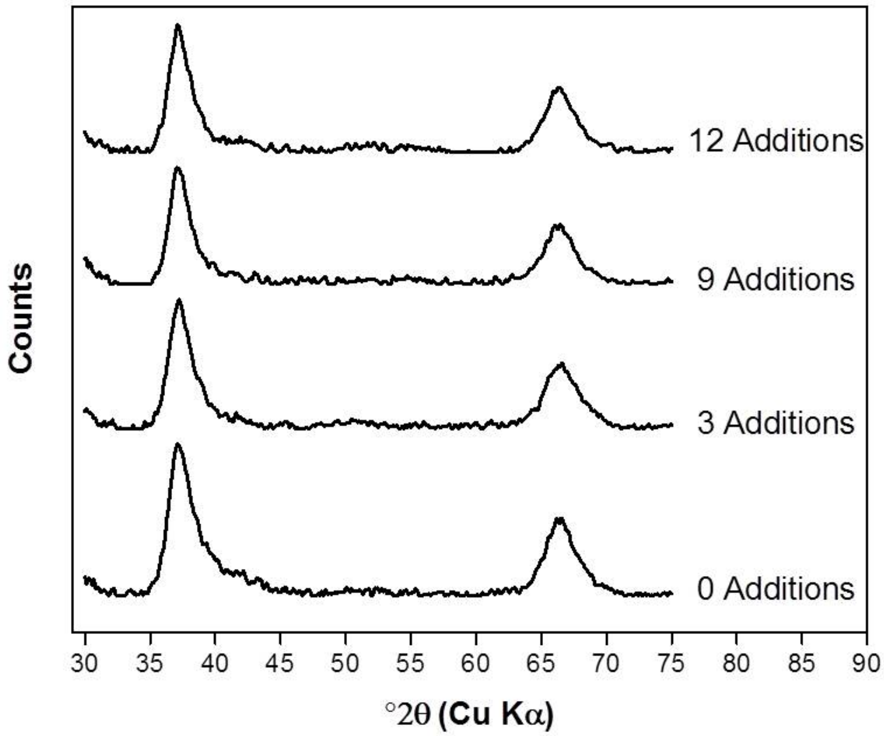

Figure S15. The crystallinity of Mn(III)-rich δ-MnO_2 during twelve additions of 80 μM BPA to 0.33 g/L Mn(III)-rich δ-MnO_2 in PIPES buffer (pH 7), as measured by XRD.

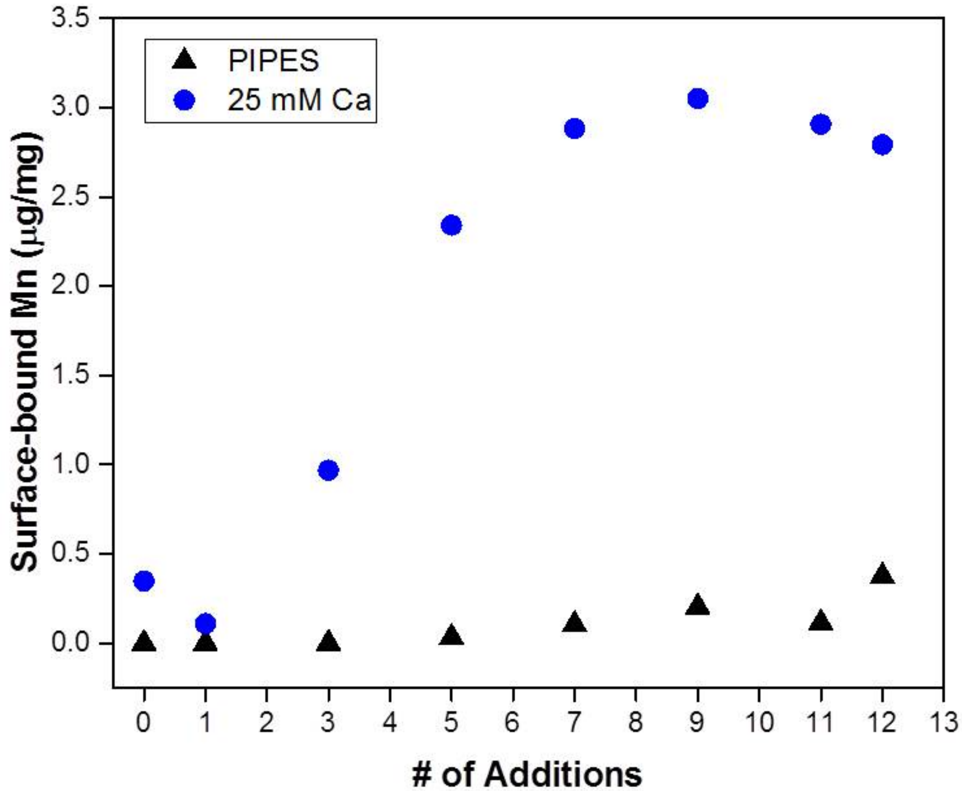

Figure S16. Surface-bound Mn extractable by a solution of 25 mM $CaCl_2$ on a Mn(III)-rich δ-MnO_2 during twelve additions of 80 µM BPA to 0.33 g/L Mn(III)-rich δ-MnO_2 in PIPES buffer (pH 7).

Table S4. EXAFS fitting results. The S_0^2 parameter was set to 0.865 for all samples.

Sample	e0	focc	S02	χ2	Shell	CN	Dist (Å)	σ2
0 Additions	6.36	0.6(1)	0.66	621	Mn-O	4	1.89(5)	0.009(6)
					Mn-O	2	1.90(4)	0.002(4)
					Mn-Mn	2	2.71(4)	0.006(4)
					Mn-Mn	4	2.85(1)	0.002(2)
					Mn-O	4	3.30(4)	0.001(4)
					Mn-O	2	3.48(9)	0.001(4)
					Mn-Na inter	2(4)	4.2(2)	0.005
					Mn-O	4	4.5(1)	0.001(7)
					Mn-O	8	4.69(8)	0.001(7)
					Mn-Mn	4	4.92(8)	0.003(2)
					Mn-Mn	2	5.0(1)	0.003(2)
					Mn-Mn	2	5.59(9)	0.002(3)
					Mn-Mn	4	5.83(5)	0.002(3)
Sample	**e0**	**focc**	**S02**	**χ2**	**Shell**	**CN**	**Dist (Å)**	**σ2**
1 Additions	5.39	0.9(1)	0.66	779	Mn-O	4	1.87(6)	0.005(7)
					Mn-O	2	1.9(1)	0.002(1)
					Mn-Mn	2	2.71(2)	0.005(1)
					Mn-Mn	4	2.86 (1)	0.002(1)
					Mn-O	4	3.35(4)	0.004(5)
					Mn-O	2	3.6(1)	0.004(5)
					Mn-Na inter	2(3)	4.1(2)	0.005
					Mn-O	4	4.4(1)	0.002(7)
					Mn-O	8	4.65(5)	0.002(7)
					Mn-Mn	4	4.89(4)	0.001(2)
					Mn-Mn	2	5.03(7)	0.001(2)
					Mn-Mn	2	5.72(8)	0.002
					Mn-Mn	4	5.82(4)	0.002
Sample	**e0**	**focc**	**S02**	**χ2**	**Shell**	**CN**	**Dist (Å)**	**σ2**
3 Additions	5.23	0.9(1)	0.66	423	Mn-O	4	1.87(6)	0.005(6)
					Mn-O	2	1.9(1)	0.002(1)
					Mn-Mn	2	2.69(1)	0.005(2)
					Mn-Mn	4	2.85(1)	0.003(1)
					Mn-O	4	3.33(5)	0.006(6)
					Mn-O	2	3.6(1)	0.006(6)
					Mn-Na inter	0(2)	4.0(6)	0.005
					Mn-O	4	4.5(1)	0.005(1)
					Mn-O	8	4.68(9)	0.005(1)
					Mn-Mn	4	4.89(2)	0.002(2)
					Mn-Mn	2	5.00(4)	0.002(2)
					Mn-Mn	2	5.70(8)	0.002
					Mn-Mn	4	5.83(5)	0.002
Sample	**e0**	**focc**	**S02**	**χ2**	**Shell**	**CN**	**Dist (Å)**	**σ2**
4 Additions	4.08	0.7(1)	0.71	316	Mn-O	4	1.87(4)	0.009(6)
					Mn-O	2	1.91(6)	0.003(1)
					Mn-Mn	2	2.72(2)	0.005(2)
					Mn-Mn	4	2.85(1)	0.002(1)
					Mn-O	4	3.35(6)	0.006(2)
					Mn-O	2	3.6(1)	0.006(2)
					Mn-Na inter	1(2)	4.1(1)	0.005
					Mn-Mn corn	0.2(2)	3.48	0.003
					Mn-O	4	4.4(1)	0.006(2)
					Mn-O	8	4.6(1)	0.006(2)
					Mn-Mn	4	4.91(6)	0.006(3)
					Mn-Mn	2	5.3(2)	0.006(3)
					Mn-Mn	2	5.6(1)	0.002

					Mn-Mn	4	5.83(3)	0.002

Sample	e0	focc	S02	χ2	Shell	CN	Dist (Å)	σ2
5 Additions	5.83	0.7(1)	0.66	841	Mn-O	4	1.87(3)	0.011(4)
					Mn-O	2	1.91(2)	0.001(1)
					Mn-Mn	2	2.71(2)	0.006(3)
					Mn-Mn	4	2.86(1)	0.003(1)
					Mn-O	4	3.41(6)	0.007(4)
					Mn-O	2	3.73(9)	0.007(4)
					Mn-Na inter	2(3)	4.0(1)	0.005
					Mn-Mn corn	0.6(3)	3.31(5)	0.003
					Mn-O	4	4.5(1)	0.004(3)
					Mn-O	8	4.69(9)	0.004(3)
					Mn-Mn	4	4.91(9)	0.005(2)
					Mn-Mn	2	5.2(2)	0.005(2)
					Mn-Mn	2	5.8(2)	0.002
					Mn-Mn	4	5.8(1)	0.002

Sample	e0	focc	S02	χ2	Shell	CN	Dist (Å)	σ2
6 Additions	6.13	0.7(1)	0.66	695	Mn-O	4	1.87(2)	0.007(2)
					Mn-O	2	1.91(3)	0.002
					Mn-Mn	2	2.75(2)	0.008(2)
					Mn-Mn	4	2.86(1)	0.003(1)
					Mn-O	4	3.23(4)	0.009(3)
					Mn-O	2	3.4(1)	0.009(3)
					Mn-Na inter	1(3)	4.1(1)	0.005
					Mn-Mn corn	0.6(2)	3.45(3)	0.003
					Mn-O	4	4.46(5)	0.005(3)
					Mn-O	8	4.67(3)	0.005(3)
					Mn-Mn	4	4.91(3)	0.005(3)
					Mn-Mn	2	5.44(5)	0.005(3)
					Mn-Mn	2	5.76(4)	0.001(1)
					Mn-Mn	4	5.86(2)	0.001(1)

Sample	e0	focc	S02	χ2	Shell	CN	Dist (Å)	σ2
7 Additions	6.42	0.9(1)	0.60	337	Mn-O	4	1.86(2)	0.006(4)
					Mn-O	2	1.93(4)	0.002
					Mn-Mn	2	2.72(2)	0.008(2)
					Mn-Mn	4	2.86(1)	0.004(1)
					Mn-O	4	3.38(3)	0.007(2)
					Mn-O	2	3.68(9)	0.007(2)
					Mn-Na inter	0(2)	4.0(2)	0.005
					Mn-Mn corn	0.4(3)	3.49(4)	0.003
					Mn-O	4	4.49(5)	0.001(1)
					Mn-O	8	4.71(3)	0.001(1)
					Mn-Mn	4	4.94(2)	0.004(1)
					Mn-Mn	2	5.19(5)	0.004(1)
					Mn-Mn	2	5.76(4)	0.002(1)
					Mn-Mn	4	5.85(2)	0.002(1)

Sample	e0	focc	S02	χ2	Shell	CN	Dist (Å)	σ2
8 Additions	6.20	0.7(1)	0.66	299	Mn-O	4	1.86(1)	0.005(2)
					Mn-O	2	1.94(3)	0.002
					Mn-Mn	2	2.70(3)	0.007(2)
					Mn-Mn	4	2.85(1)	0.002(1)
					Mn-O	4	3.30(4)	0.003(3)
					Mn-O	2	3.57(4)	0.003(3)
					Mn-Na inter	0(2)	4.10	0.005
					Mn-Mn corn	0.7(3)	3.49(7)	0.003
					Mn-O	4	4.50(7)	0.002(4)
					Mn-O	8	4.70(5)	0.002(4)
					Mn-Mn	4	4.92(5)	0.004(2)
					Mn-Mn	2	5.26(9)	0.004(2)

					Mn-Mn	2	5.81(7)	0.002(2)
					Mn-Mn	4	5.85(4)	0.002(2)

Sample	**e0**	**focc**	**S02**	**χ2**	**Shell**	**CN**	**Dist (Å)**	**σ2**
9 Additions	5.35	0.9(1)	0.66	449	Mn-O	4	1.86(2)	0.006(4)
					Mn-O	2	1.91(4)	0.002
					Mn-Mn	2	2.73(3)	0.010(3)
					Mn-Mn	4	2.85(1)	0.004(1)
					Mn-O	4	3.22(6)	0.014(8)
					Mn-O	2	3.5(1)	0.014(8)
					Mn-Na inter	1(2)	4.1(1)	0.005
					Mn-Mn corn	0.6(2)	3.43(4)	0.003
					Mn-O	4	4.42(9)	0.009(6)
					Mn-O	8	4.64(6)	0.009(6)
					Mn-Mn	4	4.91(5)	0.010(3)
					Mn-Mn	2	5.3(1)	0.010(3)
					Mn-Mn	2	5.76(4)	0.003(2)
					Mn-Mn	4	5.85(3)	0.003(2)

Sample	**e0**	**focc**	**S02**	**χ2**	**Shell**	**CN**	**Dist (Å)**	**σ2**
10 Additions	6.08	0.7(1)	0.66	421	Mn-O	4	1.86(3)	0.009(4)
					Mn-O	2	1.92(3)	0.002
					Mn-Mn	2	2.71(2)	0.006(3)
					Mn-Mn	4	2.85(1)	0.002(1)
					Mn-O	4	3.31(6)	0.005(3)
					Mn-O	2	3.60(7)	0.005(3)
					Mn-Na inter	1(3)	4.1(1)	0.005
					Mn-Mn corn	0.9(3)	3.53(7)	0.003
					Mn-O	4	4.46(9)	0.007(7)
					Mn-O	8	4.68(8)	0.007(7)
					Mn-Mn	4	4.92(6)	0.008(4)
					Mn-Mn	2	5.29(9)	0.008(4)
					Mn-Mn	2	5.75(4)	0.006(2)
					Mn-Mn	4	5.84(2)	0.006(2)

Sample	**e0**	**focc**	**S02**	**χ2**	**Shell**	**CN**	**Dist (Å)**	**σ2**
11 Additions	6.23	0.8(1)	0.66	514	Mn-O	4	1.86(1)	0.005(2)
					Mn-O	2	1.93(2)	0.002
					Mn-Mn	2	2.72(1)	0.007(2)
					Mn-Mn	4	2.86(1)	0.003(1)
					Mn-O	4	3.33(3)	0.004(2)
					Mn-O	2	3.64(4)	0.004(2)
					Mn-Na inter	0.37 ± 1.11	4.1(1)	0.005
					Mn-Mn corn	1.1(3)	3.52(2)	0.003
					Mn-O	4	4.23(3)	0.013(6)
					Mn-O	8	4.56(5)	0.013(6)
					Mn-Mn	4	4.88(4)	0.008(3)
					Mn-Mn	2	5.29(9)	0.008(3)
					Mn-Mn	2	5.82(3)	0.003(1)
					Mn-Mn	4	5.83(9)	0.003(1)

Sample	**e0**	**focc**	**S02**	**χ2**	**Shell**	**CN**	**Dist (Å)**	**σ2**
12 Additions	5.76	0.7(1)	0.66	379	Mn-O	4	1.87(2)	0.008(3)
					Mn-O	2	1.91(3)	0.002
					Mn-Mn	2	2.72(2)	0.008(2)
					Mn-Mn	4	2.85(1)	0.003(1)
					Mn-O	4	3.29(7)	0.003(2)
					Mn-O	2	3.62(3)	0.003(2)
					Mn-Na inter	1(2)	4.1(1)	0.005
					Mn-Mn corn	1.3(2)	3.49(2)	0.003
					Mn-O	4	4.48(8)	0.004(5)
					Mn-O	8	4.70(4)	0.004(5)

Mn-Mn	4	4.94(4)	0.004(2)
Mn-Mn	2	5.22(6)	0.004(2)
Mn-Mn	2	5.79(5)	0.002(1)
Mn-Mn	4	5.85(3)	0.002(1)

References

(1) Nakamura, S.; Tezuka, Y.; Ushiyama, A.; Kawashima, C.; Kitagawara, Y.; Takahashi, K.; Ohta, S.; Mashino, T. Ipso substitution of bisphenol A catalyzed by microsomal cytochrome P450 and enhancement of estrogenic activity. *Toxicol. Lett.* **2011**, *203* (1), 92–95.

(2) Im, J.; Prevatte, C. W.; Campagna, S. R.; Löffler, F. E. Identification of 4-hydroxycumyl alcohol as the major MnO_2-mediated bisphenol A transformation product and evaluation of its environmental fate. *Environ. Sci. Technol.* **2015**, *49* (10), 6214–6221.